Conformational Changes in the Active Site Loops of Dihydrofolate Reductase during the Catalytic Cycle†

Rani P. Venkitakrishnan,‡ Eduardo Zaborowski,‡ Dan McElheny,‡ Stephen J. Benkovic,§ H. Jane Dyson,‡ and Peter E. Wright*,‡

Department of Molecular Biology and Skaggs Institute for Chemical Biology, The Scripps Research Institute, La Jolla, California 92037, and Department of Chemistry, The Pennsylvania State University, University Park, Pennsylvania 16802

Received August 31, 2004; Revised Manuscript Received October 7, 2004

ABSTRACT: *Escherichia coli* dihydrofolate reductase (DHFR) has several flexible loops surrounding the active site that play a functional role in substrate and cofactor binding and in catalysis. We have used heteronuclear NMR methods to probe the loop conformations in solution in complexes of DHFR formed during the catalytic cycle. To facilitate the NMR analysis, the enzyme was labeled selectively with [^{15}N]-alanine. The 13 alanine resonances provide a fingerprint of the protein structure and report on the active site loop conformations and binding of substrate, product, and cofactor. Spectra were recorded for binary and ternary complexes of wild-type DHFR bound to the substrate dihydrofolate (DHF), the product tetrahydrofolate (THF), the pseudosubstrate folate, reduced and oxidized NADPH cofactor, and the inactive cofactor analogue 5,6-dihydroNADPH. The data show that DHFR exists in solution in two dominant conformational states, with the active site loops adopting conformations that closely approximate the occluded or closed conformations identified in earlier X-ray crystallographic analyses. A minor population of a third conformer of unknown structure was observed for the apoenzyme and for the disordered binary complex with 5,6-dihydroNADPH. The reactive Michaelis complex, with both DHF and NADPH bound to the enzyme, could not be studied directly but was modeled by the ternary folate:NADP$^+$ and dihydrofolate:NADP$^+$ complexes. From the NMR data, we are able to characterize the active site loop conformation and the occupancy of the substrate and cofactor binding sites in all intermediates formed in the extended catalytic cycle. In the dominant kinetic pathway under steady-state conditions, only the holoenzyme (the binary NADPH complex) and the Michaelis complex adopt the closed loop conformation, and all product complexes are occluded. The catalytic cycle thus involves obligatory conformational transitions between the closed and occluded states. Parallel studies on the catalytically impaired G121V mutant DHFR show that formation of the closed state, in which the nicotinamide ring of the cofactor is inserted into the active site, is energetically disfavored. The G121V mutation, at a position distant from the active site, interferes with coupled loop movements and appears to impair catalysis by destabilizing the closed Michaelis complex and introducing an extra step into the kinetic pathway.

Dihydrofolate reductase (DHFR)[1] (5,6,7,8-tetrahydrofolate: NADP$^+$ oxidoreductase, EC 1.5.1.3) utilizes NADPH to reduce 7,8-dihydrofolate (DHF) to form the product 5,6,7,8-tetrahydrofolate (THF). DHFR plays a central role in maintenance of the cellular pools of THF and its derivatives, which are essential for purine and thymidylate biosynthesis and hence for cell growth, and is a target for several anticancer and antibacterial drugs (*1*, *2*). *E. coli* DHFR has been the subject of intensive structural and mechanistic studies (see ref *3* for a recent review). The kinetics of the wild-type enzyme have been thoroughly investigated, resulting in a complete description of the overall kinetic pathway (*4*). The kinetic intermediates in the catalytic cycle under cellular conditions of substrate and cofactor concentration are shown in Figure 1a, and the chemical structures of the various substrates, products, and cofactors are shown in Figure 1b. Binding of DHF substrate to the holoenzyme (the binary complex with reduced NADPH cofactor, henceforth denoted E:NADPH) leads to formation of the ternary Michaelis complex (E:DHF:NADPH) which, following hydride transfer, forms the ternary product complex (E:THF:NADP$^+$). Dissociation of the oxidized cofactor leads to formation of the product binary complex E:THF, which then rebinds NADPH to form the product release complex (E:THF:NADPH). The fundamental chemical event, hydride transfer from NADPH to dihydrofolate, occurs at a rate of $\sim 10^3$ s^{-1} at pH 6−7 and is not rate-limiting under these

† This work was supported by Grant GM56879 from the National Institutes of Health. E.Z. was the recipient of a Rothschild Foundation postdoctoral fellowship.

* Corresponding author. Address: Department of Molecular Biology, The Scripps Research Institute, 10550 North Torrey Pines Rd, La Jolla CA 92037. Phone: 858 784 9721. Fax: 858 784 9822. E-mail: wright@scripps.edu.

‡ The Scripps Research Institute.

§ The Pennsylvania State University.

[1] Abbreviations: DHFR, dihydrofolate reductase; DHF, 7,8-dihydrofolate; THF, 5,6,7,8-tetrahydrofolate; NADP$^+$, nicotinamide adenine dinucleotide phosphate; NADPH, reduced nicotinamide adenine dinucleotide phosphate; DHNADPH, 5,6-dihydroNADPH; nuclear magnetic resonance, NMR; HSQC, heteronuclear single quantum correlation.

10.1021/bi048119y CCC: $27.50
Published on Web 11/25/2004

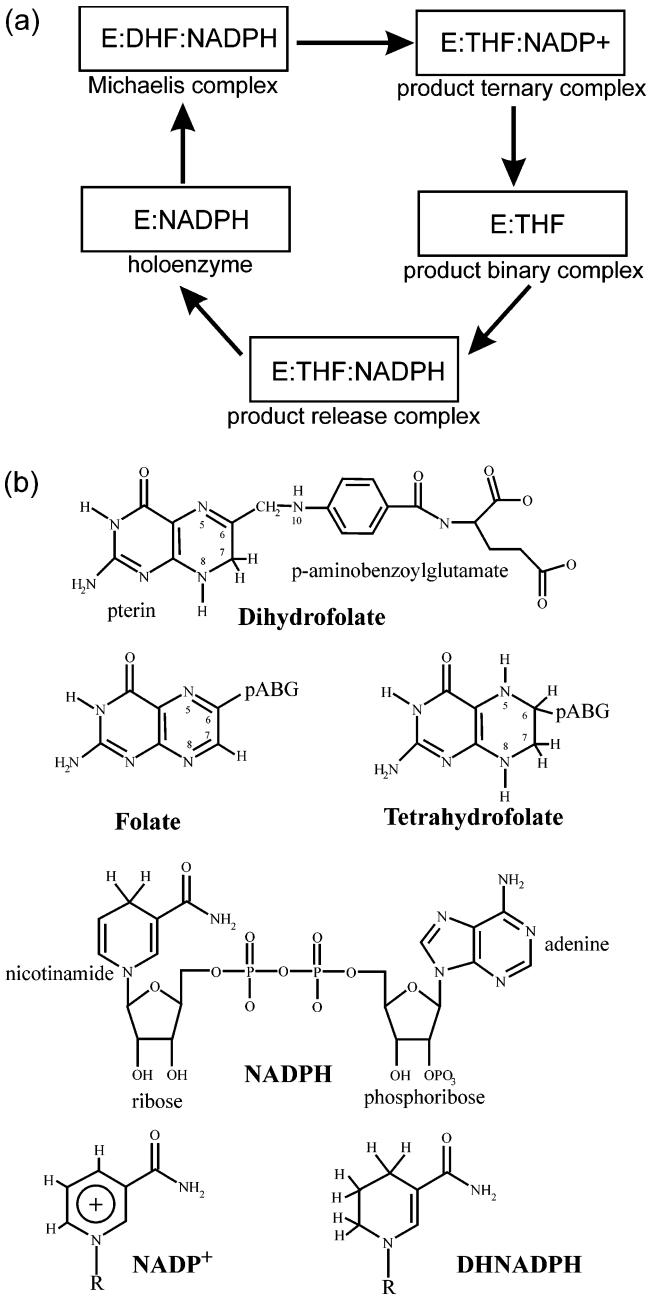

FIGURE 1: (a) Simplified catalytic cycle for DHFR, derived from ref *4*. (b) Chemical structures of the substrates, cofactors, and analogues used in the present studies.

conditions (*4*). Rather, the rate-limiting step is a physical process, tetrahydrofolate release, which occurs preferentially after NADPH replaces $NADP^+$ in the ternary product complex. Identical or highly similar kinetic schemes have been found for the *Lactobacillus casei* and mouse DHFRs (*5*, *6*).

X-ray structures have been determined for more than 50 complexes of *E. coli* DHFR with various ligands. The protein fold (Figure 2) consists of an eight-stranded β-sheet formed of β-strands βA to βH, four α-helices (designated αB, αC, αE, and αF), and five loops (*7*). The substrate and cofactor bind in a 15 Å deep hydrophobic cleft that contains only a single hydrophilic residue, Asp27. The hydride donor atom, C_4 of the NADPH cofactor, and the C_6 hydride acceptor atom on DHF are in van der Waals contact (*8*). The active site cleft divides the protein into two structural domains, with K38 and V88 functioning as a hinge (*9*). The major domain is formed by residues 1−37 and 89−159 and provides many residues critical for substrate binding. The smaller domain (residues 38−88) binds the adenosine moiety of the cofactor and is termed the adenosine-binding domain. Hinge motions cause the adenosine binding domain to move relative to the major domain upon binding of various ligands, resulting in closure of the cleft that binds the (*p*-aminobenzoyl)-L-glutamate tail of the substrate (*9*).

Conformational changes are also observed in three loops in the major domain of the protein upon binding of ligands to apo-DHFR (*9*). These are the Ala9−Asn23 loop connecting βA and αB (termed the Met20 loop by Sawaya and Kraut (*10*)), and the loops connecting βF and βG (residues Ala117−Asp131) and βG and βH (residues Asp142-His149) (designated the FG and GH loop, respectively). The Met20 loop serves as a "gate or lid", which closes over the pteridine and nicotinamide rings of the bound folate and cofactor. From their detailed analysis of the numerous X-ray structures of *E. coli* DHFR, Sawaya and Kraut (*10*) have identified three conformations of the Met20 loop, termed open, closed, and occluded. The open conformation is ligand-independent and is observed in space groups where the Met20 loop participates in lattice contacts. In space groups where lattice contacts involving the Met20 loop are weak or absent, the enzyme adopts the closed or occluded conformation, depending on the nature of the bound ligands. The occluded conformation occurs only when the binding pocket for the nicotinamide-ribose moiety of the cofactor is empty; in this conformation, residues 14−16 of the Met20 loop protrude into the pocket and prevent binding of the nicotinamide ring. In the closed conformation, the Met20 loop packs tightly against the nicotinamide-ribose and seals the active site. The loop conformational transitions are accompanied by changes in hydrogen bonding to the FG and GH loops (*10*). The closed and occluded conformations have also been observed in solution by NMR (*11*).

On the basis of numerous X-ray structures of *E. coli* DHFR complexes, Sawaya and Kraut (*10*) have proposed a structural model for the conformational changes that occur during the catalytic cycle. Due to the instability of the substrate, product, and cofactor, stable analogues were used to model many of the intermediate complexes in the reaction cycle. The structures suggest that the Met20 loop adopts the closed conformation, with the nicotinamide ring positioned in the active site, in the holoenzyme (E:NADPH), the Michaelis complex, and the transition state. On the basis of the structures of complexes with product analogues, Sawaya and Kraut propose that, following hydride transfer, the nicotinamide ring is excluded from the binding pocket due to steric clash with the puckered pterin ring of THF, and they suggest that the remaining complexes in the reaction cycle are therefore in the occluded conformation (*10*).

In the course of NMR studies of the structure and dynamics of complexes of *E. coli* DHFR with the substrate analogue folate, with NADPH, and with folate plus cofactor or a cofactor analogue (*11*−*13*), we have identified a number of chemical shift markers for the closed and occluded Met20 loop conformations and for the presence of the pterin and nicotinamide rings within the binding pocket. In the present work, we use NMR to probe directly the active site loop conformation for all intermediates in the catalytic cycle, with

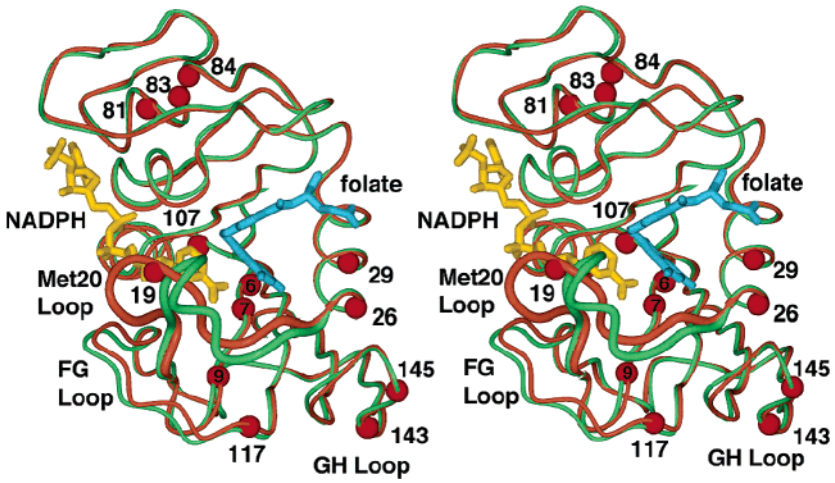

FIGURE 2: Stereoview of the superposition of the backbones of X-ray crystal structures of DHFR (*10*) in complex with folate (PDB 1rx7, green) and with $NADP^+$ and folate (PDB 1rx2, pink). Folate and $NADP^+$ in the 1rx2 structure are shown in blue and yellow, respectively. The backbone N atoms of the alanine residues are shown as red spheres. The Met20 loop is represented by thicker lines to emphasize the conformational change between the occluded and closed states.

the sole exception of the E:DHF:NADPH Michaelis complex, which reacts too rapidly to permit NMR measurements. To facilitate these measurements and circumvent the need for making complete backbone resonance assignments for each complex, DHFR was labeled selectively with [^{15}N]alanine or [^{13}C,^{15}N]alanine to yield highly simplified subspectra containing only alanine backbone NH resonances. Alanine was chosen for labeling because of its high abundance in the *E. coli* DHFR sequence, because the Ala amide resonances are well-resolved, and because several Ala resonances are sensitive reporters of the active site loop conformations and the presence of cofactor and substrate in their binding pockets. Our NMR experiments confirm the Sawaya and Kraut model (*10*) for the conformational changes occurring during the catalytic cycle, provide new insights into the interactions of DHFR with substrate and ligands, and suggest a mechanism by which mutations at Gly121 in the FG loop impair the catalytic activity of the enzyme.

MATERIALS AND METHODS

Sample Preparation. E. coli BL21 (DE3) cells were transformed with the expression plasmid containing the DHFR and carbenicillin resistance gene. Both wild-type enzyme and the G121V mutant were expressed by growing the cells on M9 medium containing glucose (2 g/L), [^{15}N]-Alanine (75 mg/L), and a mixture of all other 19 unlabeled amino acids in proportion to their average abundance in cells (total 1.925 g/L). The expressed DHFR contains selectively ^{15}N-labeled alanine at positions 6, 7, 9, 19, 26, 29, 81, 83, 84, 107, 117, 143, and 145. Wild-type DHFR was also expressed as above using ^{13}C,^{15}N-labeled alanine. Both wild-type and mutant enzyme were purified by previously described methods (*14*, *15*). The amount of protein was estimated spectrophotometrically using an extinction coefficient of 31 100 M^{-1} cm^{-1} at 280 nm.

Due to the oxygen and light sensitivity of the cofactor and substrate used in the investigations, NMR sample buffer [70 mM potassium phosphate (pH 7.6), 25 mM KCl in 93% H_2O/7% D_2O, containing 0.02% sodium azide and 1 mM DTT] was thoroughly degassed in a vacuum by several freeze−thaw cycles. The protein samples were exchanged into the NMR buffer using an Amicon NAP5 column in an argon-equilibrated glovebox. The protein concentration was 1 mM for all NMR experiments, and a 4−40-fold excess of substrate/product or cofactor and their analogues was used. NMR samples were subjected to an additional freeze−thaw cycle and stored in argon atmosphere. Amberized NMR tubes equipped with Teflon valves for connecting to the vacuum manifold were used wherever necessary.

NMR Spectroscopy. NMR spectra were acquired at 282 K on Bruker DRX600 and AMX600 spectrometers equipped with 5 mm triple resonance probes with single axis or triple axis gradients. The probe temperature was calibrated using neat methanol. Spectra of the DHNADPH complexes were acquired at 287 K on a Bruker Avance 500 spectrometer equipped with a cryoprobe.

2D ^{1}H−^{15}N HSQC spectra were recorded on the various enzyme complexes with 2048 complex data points in t_2 and a variable number of data points (160−256) in the t_1 dimension and with 128 transients per experiment. Spectra were processed using NMRPIPE (*16*) and analyzed using NMRVIEW (*17*). Data sets were zero-filled to 4096 points in ω_2 and 1024 points in the ω_1 dimension and apodized with sine bell or shifted sine bell window functions prior to processing. The ^{1}H chemical shifts were referenced to internal 2,2-dimethyl-2-silapentane-5-sulfonate (DSS). The ^{15}N dimension was referenced indirectly (*18*). HNCO spectra (*19*) were acquired at 282 K on samples of wild-type DHFR labeled with [^{13}C,^{15}N]alanine. 1D HNCO spectra were recorded with 4096 transients, and 2D spectra were typically acquired with 2048 complex data points in t_2, 32 data points in the t_1 dimension, and 1024 transients per experiment.

RESULTS

^{1}H−^{15}N HSQC spectra were recorded for complexes of wild-type and the G121V mutant DHFR to probe the conformation of the intermediates formed in the catalytic cycle. To simplify the HSQC spectra and facilitate assignment of resonances, the protein was labeled specifically with [^{15}N]alanine. The 13 alanine residues are distributed throughout the protein structure, with several (Ala6, Ala7, Ala9, Ala19, Ala26, Ala29, and Ala117) located in the active site

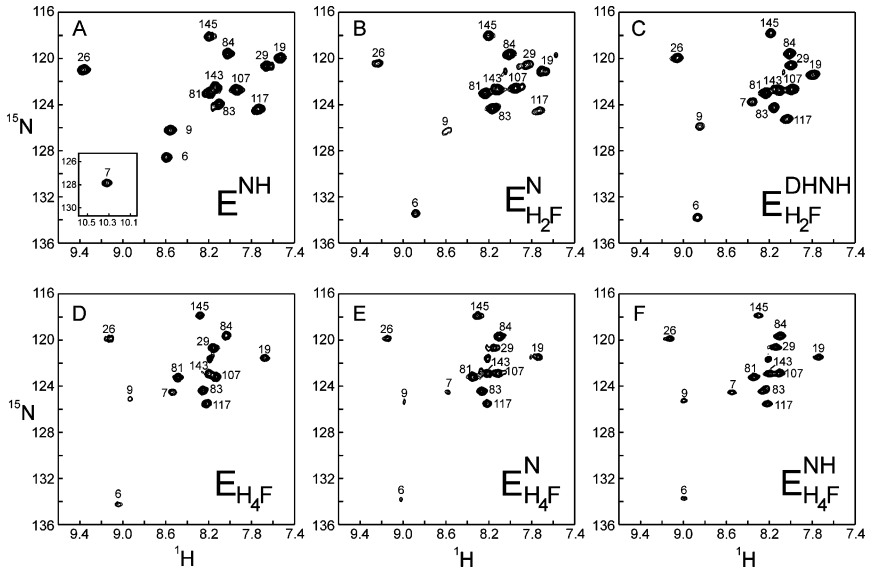

FIGURE 3: Representative ^{1}H−^{15}N HSQC spectra of [^{15}N]alanine-labeled DHFR complexes. The assignments for the alanine resonances are indicated. (A) E:NADPH; (inset) low field-shifted cross-peak of Ala7. (B) E:DHF:NADP^{+} (no cross-peak is visible for Ala7). (C) E:DHF:DHNADPH. (D) E:THF. (E) E:THF:NADP^{+}. (F) E:TFH:NADPH. The spectra in panels A−C were acquired at 287 K and those in panels D−F at 282 K.

loops or substrate and cofactor binding sites (Figure 2). Assignments of the cross-peaks for the alanine residues were based on assignments for the occluded E:folate and E:folate:DHNADPH complexes and the closed E:folate:NADP^{+} and E:NADPH complexes made previously using triple resonance methods (*11*, *12*, *20*). Representative spectra of the wild-type DHFR complexes are shown in Figure 3.

Most of the alanine resonances shift only slightly between complexes and can readily be assigned by inspection of the pattern of shifts. On the other hand, the ^{1}HN and ^{15}N resonances of Ala7, which is located within the active site, are extremely sensitive to the nature of the bound ligands. The NH and carbonyl groups of Ala7 form hydrogen bonds to the carboxamide group of the nicotinamide ring of the cofactor in the closed E:NADPH and E:folate:NADP^{+} complexes, in which the nicotinamide-ribose occupies its binding pocket within the active site (*8*, *10*). To obtain unambiguous assignments for the Ala7 ^{1}HN resonance in several of the complexes, DHFR was labeled with [^{13}C,^{15}N]-alanine and 1D or 2D HNCO spectra were recorded. There are two occurrences of adjacent alanine residues in DHFR, Ala6-Ala7, and Ala83-Ala84. Of the 13 alanine residues in DHFR, only Ala7 and Ala84 form peptide bonds in which the ^{15}N is bonded directly to a ^{13}C-labeled carbonyl (the ^{13}CO of Ala6 and Ala83); thus, only the Ala7 and Ala84 amide resonances are observed in the HNCO spectrum, in which magnetization is transferred from the carbonyl carbon of the first Ala to the ^{15}N of the second Ala in each adjacent pair. Representative 1D HNCO spectra are shown in Figure 4.

Spectra were recorded for [^{15}N]Ala-labeled wild-type DHFR in the following complexes: apo-DHFR, E:folate, E:DHF, E:THF, E:NADPH, E:NADP^{+}, E:DHNADPH, E:folate:NADPH, E:folate:NADP^{+}, E:DHF:DHNADPH, E:DHF:NADP+, E:THF:NADPH, and E:THF:NADP^{+}. The variations in Ala ^{1}HN and ^{15}N chemical shifts are summarized as histograms in Figure 5 and the numerical values and assignments are tabulated in the Supporting Information. Since folate acts as a substrate, albeit a poor one, for DHFR, HSQC spectra for the E:folate:NADPH complex were recorded immediately after mixing. The spectra remained unchanged for a period of 1 h, but after 2 h product resonances were detectable and grew in intensity until the reaction was complete after a few hours at 282 K.

^{1}H−^{15}N HSQC spectra were recorded for the apoenzyme, the folate, DHF, and NADPH binary complexes, and the folate:NADPH, folate:NADP^{+}, and THF:NADPH ternary complexes of the G121V mutant DHFR. Representative spectra are shown in Figure 6 and the Ala ^{1}HN and ^{15}N chemical shifts are summarized in Figure 7. Detailed assignments and numerical values are given as Supporting Information.

DISCUSSION

Our previous analysis of chemical shifts in the E:folate, E:NADPH, E:folate:DHNADPH, and E:folate:NADP^{+} complexes led to identification of numerous resonances that are markers of the closed−occluded Met20 loop conformational transition, of substrate and cofactor binding, and of the presence of the nicotinamide ring in the active site binding pocket (*13*). These studies provide a framework for interpretation of the chemical shift changes observed for the alanine ^{1}HN and ^{15}N resonances in the present work. The ^{15}N resonance of Ala6 is sensitive to the location of the pterin ring of the bound substrate or product; it is shifted downfield by ∼7 ppm when DHF or THF replace folate in the pterin binding pocket. The ^{15}N and ^{1}H resonances of the Ala7 amide primarily reflect hydrogen-bonding interactions with the carboxamide group of the nicotinamide moiety of bound cofactor (although they are also sensitive to bound substrate); the ^{1}HN resonance is shifted downfield by ∼1−2 ppm when the nicotinamide ring occupies the active site in the closed E:NADPH or E:folate:NADP^{+} complexes. The Ala117 amide resonances are a reliable marker of the closed−occluded conformational transition, with the ^{1}HN resonance shifting ∼0.4 ppm upfield upon formation of closed complexes. The NH cross-peaks of Ala9 and Ala19 are sensitive to both cofactor and substrate binding, as well as to the

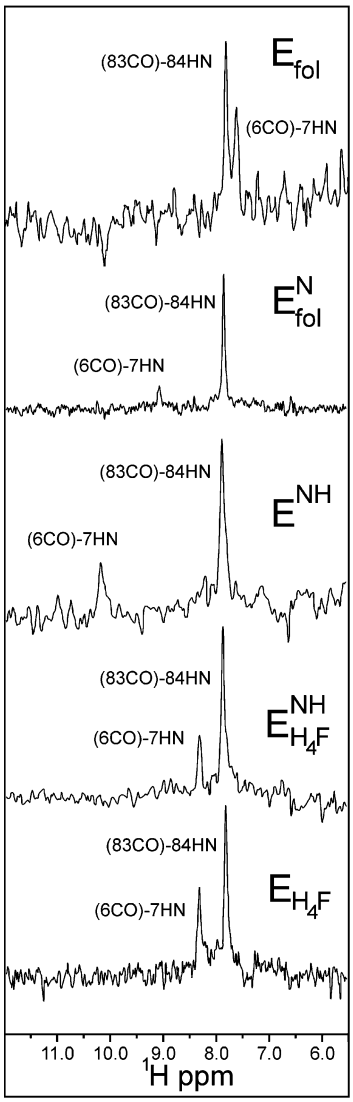

FIGURE 4: Representative 1D HNCO spectra of DHFR labeled with [^{15}N,^{13}C]alanine. Only the second of a consecutive pairs of alanines (i.e. Ala7 and Ala 84) gives a peak in these spectra. From the top, the complexes are E:folate, E:folate:NADP$^+$, E:NADPH, E:THF:NADPH, and E:THF.

Met20 loop conformation; those of Ala26 and Ala29 reflect the loop conformational change and binding of folate but are insensitive to cofactor, while the amide ^{1}HN resonance of Ala81 undergoes a small upfield shift on binding of cofactor. The remaining alanine amide resonances (Ala83, Ala84, Ala107, Ala143, and Ala145) are little perturbed by substrate or cofactor binding or by Met20 or FG loop conformational changes.

Conformational Changes in Wild-Type DHFR. The binary complexes of DHFR with folate and NADPH adopt the occluded and closed Met20 loop conformations, respectively (*10*). The ^{1}H−^{15}N HSQC spectra of these complexes, obtained using ^{15}N-alanine labeled DHFR, are shown in Figure 3 and the ^{1}H and ^{15}N chemical shifts are summarized in Figure 5. For the E:folate:NADP$^+$ complex, the ^{1}HN and ^{15}N chemical shifts of Ala117 are nearly identical to those of the E:NADPH complex, in accord with its fully closed Met20 loop conformation (*10, 11*). The ^{1}HN resonances of Ala81 and Ala107 are shifted upfield and that of Ala84 is shifted downfield in the spectra of the E:NADPH and E:folate:NADP$^+$ complexes relative to that of E:folate, reflecting binding of the adenosine moiety of the cofactor. The large downfield shifts observed for both the ^{1}HN and ^{15}N resonances of the Ala7 amide (Figure 5) provide direct evidence that the nicotinamide ring occupies the binding pocket in the E:NADPH and E:folate:NADP$^+$ complexes in solution, as observed in the X-ray structures.

The HSQC spectrum of the E:THF product binary complex is shown in Figure 3D. The ^{1}HN and ^{15}N chemical shifts of Ala117 are very similar to those for E:folate, showing that the THF binary complex is in the occluded conformation, as predicted by Sawaya and Kraut (*10*) on the basis of X-ray structures of the binary dideazatetrahydrofolate, a THF analogue, complex. Indeed, the only resonances that display significant differences (>0.05 ppm for ^{1}H, >0.2 ppm for ^{15}N) in chemical shift between the folate and THF binary complexes are those of Ala6, Ala7, Ala9, and Ala19. The largest resonance shifts are observed for residues 6 and 7, the amides of which are in van der Waals contact with atoms of the pterin ring (*10*). The large downfield shift of the ^{15}N resonance of Ala6 in the DHF and THF complexes reflects formation of a hydrogen bond between the protonated N8 of the pterin ring and the backbone carbonyl of Ile5 (*8*); this hydrogen bond cannot be formed by folate. It is of interest that small backbone conformational differences occur in the region of Ala19 (residues 16−21) in the X-ray structures of the binary folate and dideazatetrahydrofolate complexes (PDB 1rx5 and 1rx7), even though the Met20 loop is clearly in the occluded conformation in both complexes, and are probably responsible for the changes in the Ala19 chemical shift. The spectrum of the E:DHF binary complex (not shown) is very similar to that of the E:THF complex, confirming that it too is in the occluded conformation and that the pterin ring occupies its binding pocket.

Binding of NADP$^+$ or NADPH to E:THF to form the E:THF:NADP$^+$ product ternary complex and the E:THF:NADPH product release complex results in only very small changes in the [^{15}N]Ala HSQC spectrum (Figure 3E,F). A 0.14 ppm upfield shift in the ^{1}HN resonance of Ala81, together with small shift changes for Ala84 and Ala107, confirms binding of the adenosine moiety of the cofactor to the enzyme. The ^{1}H and ^{15}N chemical shifts of Ala117 are invariant between the three complexes, showing that the Met20 loop adopts the occluded conformation in all of them. In this conformation, the backbone of Gly15 and the side chain of Met16 are inserted into the active site cleft, where they occlude the nicotinamide-ribose binding pocket and prevent insertion of the nicotinamide ring into the active site (*10*). The absence of significant shift changes for Ala7 resonances, which are exquisitely sensitive to the presence of bound nicotinamide, confirms that the nicotinamide ring is excluded from its binding pocket in both the E:THF:NADP$^+$ and E:THF:NADPH complexes, even though the adenosine moiety of the cofactor remains tightly bound to the enzyme. Thus, using NMR, we are able to characterize directly the active site conformation in the product ternary, product binary, and product release complexes: the Met20 loop is seen to be occluded, with the nicotinamide ring excluded from the binding pocket, as was deduced from the X-ray structures of model complexes with a THF analogue (*10*).

The rapid reduction of the substrate DHF by the holoenzyme (E:NADPH) precludes direct NMR studies of the

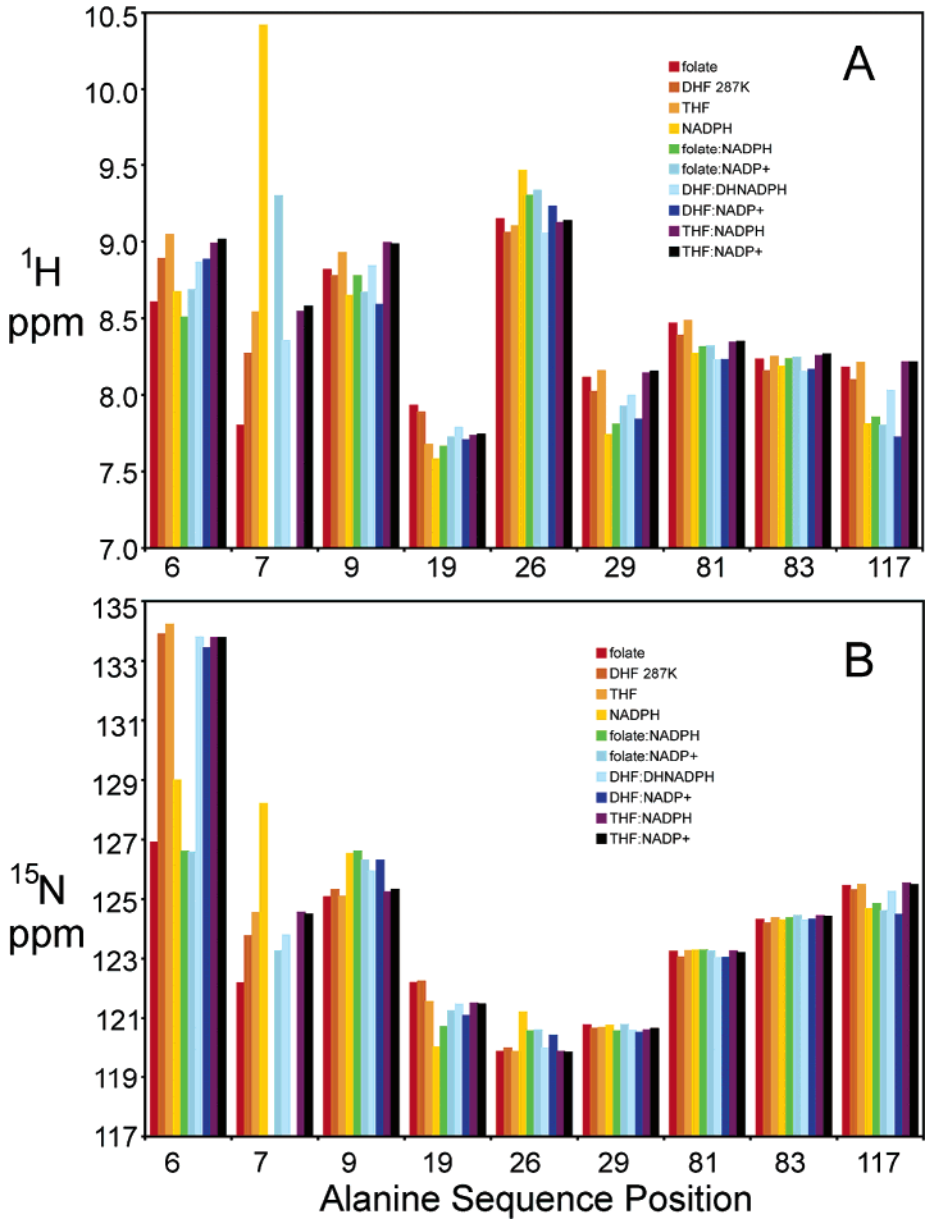

FIGURE 5: Histograms summarizing (A) ^{1}HN and (B) ^{15}N chemical shifts of representative alanine residues in wild-type DHFR complexes. Complete data for all complexes are available in Supporting Information. Complexes are represented by red, E:folate; dark orange, E:DHF; orange, E:THF; yellow, E:NADPH; green, E:folate:NADPH; aqua, E:folate:NADP$^+$; light blue, E:DHF:DHNADPH; dark blue, E:DHF:NADP$^+$; purple, E:THF:NADPH; black, E:THF:NADP$^+$. All chemical shifts refer to spectra recorded at 282 K, except for those of the E:DHF and E:DHF:DHNADPH complexes for which data were recorded at 287 K.

substrate ternary complex. The Michaelis complex was therefore modeled using the substrate analogue folate, which is reduced more slowly, in place of DHF. The HSQC spectrum of a freshly prepared sample of [^{15}N]Ala-labeled E:folate:NADPH, recorded within 1 h, before appreciable reaction had occurred, is very similar to that of E:folate:NADP$^+$ (shown in ref *13*), showing that the complex adopts the closed conformation. The Michaelis complex was also "modeled" using ternary DHFR complexes formed from the substrate DHF and unreactive forms of the cofactor—NADP$^+$ and 5,6-dihydroNADPH (Figure 3B,C). Like the corresponding complexes with the substrate analogue folate, the E:DHF:NADP$^+$ complex adopts the closed conformation, while the E:DHF:DHNADPH complex is predominantly occluded. Upon contouring the E:DHF:DHNADPH HSQC spectrum to low levels, very weak cross-peaks are observed at the positions expected for Ala26 and Ala117 in the closed form, suggesting that a few percent of the closed conformation exists in equilibrium with the dominant occluded state.

In the HSQC spectrum of the [^{15}N]alanine-labeled E:NADP$^+$ binary complex (not shown), resonances of many of the alanine residues in the active site and surrounding loops are severely broadened and some resonances (of Ala19, 29, 117) are observed at intermediate chemical shifts, between those of the closed and occluded forms. This is probably associated with fluctuations of the ribose-nicotinamide moiety in to and out of the binding cleft; complete dissociation of NADP$^+$ is unlikely, since the resonances of Ala81, Ala83, and Ala84 show little broadening and confirm that the adenosine moiety of the cofactor is fully bound. The nicotinamide mononucleotide moiety and residues 16−20 of the Met20 loop were found to be disordered in the X-ray

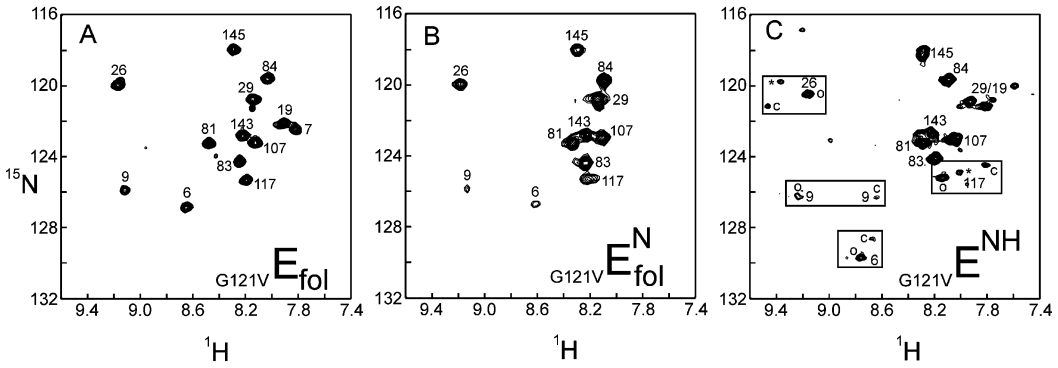

FIGURE 6: Representative $^{1}H-^{15}N$ HSQC spectra of [^{15}N]alanine-labeled G121V mutant DHFR. The assignments for the alanine resonances are indicated. (A) E:folate. (B) E:folate:$NADP^+$. (C) E:NADPH. The boxed regions in panel C highlight the resonances of Ala6, Ala9, Ala26, and Ala117, which are split due to population of both the occluded and closed states (indicated by O and C, respectively). A minor cross-peak observable for Ala26 and Ala117 (marked with an asterisk) indicates formation of a small population of a third conformational state.

structure of the E:$NADP^+$ complex; this disorder has been attributed to a tendency for the nicotinamide ring to occupy two sites, one in the binding pocket and the other in the bulk solvent (*8*, *10*). Conformational disorder is also evident in the spectra of the E:DHNADPH complex, with multiple resonances observed for residues 6, 9, 19, 26, 29, and 117 (data not shown). However, in this case, there appears to be little broadening, and cross-peaks are observed in the HSQC spectrum at chemical shifts characteristic of both the occluded state and a smaller population of the closed conformation. In addition, the presence of a significant population of a third unidentified conformer is evident from an additional cross-peak associated with each of the alanine residues listed above.

Disorder in the active site region of the [^{15}N]alanine-labeled apoenzyme is evident in the HSQC spectrum, with obvious doubling of the cross-peaks for alanines 6, 9, 26, and 117. For each alanine, one cross-peak has ^{1}H and ^{15}N chemical shifts close to those of the occluded conformation while the other appears to arise from a small population of an unrecognized conformational state. Interestingly, the cross-peaks associated with the minor conformer are at very similar chemical shifts to those of the third conformer observed in the DHNADPH complex. While the nature of this state is unknown, it is tempting to speculate that it might be related to the third conformational state, the "open" Met20 loop conformation, observed in the crystal structures in certain space groups where it is stabilized by crystal contacts (*10*). Heterogeneity in the apoenzyme has also been observed in previous NMR and kinetics experiments (*4*, *21*, *22*), and the absence of electron density for the Met20 loop in the X-ray structure of apo-DHFR has been interpreted in terms of dynamic conformational averaging (*9*, *10*). The rate of conformational exchange in the Met20 loop of apoDHFR has been determined to be ca. 35 s^{-1} (*22*).

The conformation of the active site loops in each of the complexes is summarized in Table 1. When only the substrate binding site is occupied, as in the binary E:folate, E:DHF, or E:THF complexes, the Met20 loop is occluded. In the occluded conformation, the backbone in the central region of the Met20 loop and the side chain of Met16 project into the active site and sterically occlude the binding pocket for the nicotinamide-ribose group of the cofactor (*10*). When the nicotinamide-ribose occupies its binding pocket, as in the holoenzyme (E:NADPH, Figure 3A), the Met16 side chain is flipped out of the active site and the Met 20 loop closes over the cofactor and seals the active site (*10*). These Met20 loop conformational changes involve large movements of both the backbone and side chains (Figure 2). The E:folate:$NADP^+$, E:folate:NADPH, and E:DHF:$NADP^+$ ternary complexes also adopt the closed conformation, with both the pterin and nicotinamide rings in the active site. However, when either the pterin or nicotinamide ring is strongly puckered, as in THF or DHNADPH, the loop conformation is occluded and the nicotinamide ring is excluded from the active site (as confirmed by the chemical shift of the Ala7 NH cross-peak). This is observed in the ternary E:folate:DHNADPH, E:DHF:DHNADPH (Figure 3C), E:THF:NADPH (Figure 3F), and E:THF:$NADP^+$ (Figure 3E) complexes. It is notable that the adenosine moiety of the cofactor remains bound to the enzyme in these occluded complexes, even though the nicotinamide ring is not bound in the active site, as evidenced by the chemical shift of Ala81.

The chemical shift of the Ala6 resonance shows that the pterin ring occupies the active site in all complexes containing folate, DHF, or THF, in both the closed and occluded conformations and irrespective of whether the ring is planar or strongly puckered. The pterin ring thus appears to have a stronger propensity to bind in the active site than does the nicotinamide ring of the cofactor. Even in the binary cofactor complexes, nicotinamide ring pucker (DHNADPH) or charge ($NADP^+$) leads to conformational disorder and partial occupancy of the nicotinamide binding site. For the E:DHNADPH complex, both closed (ring in) and occluded (ring out) conformations are observed, together with a third unidentified conformer with resonances at intermediate chemical shifts. Broadening of many of the active site resonances and loop conformational marker resonances in the E:$NADP^+$ complex suggests dynamic exchange between the closed and occluded conformations; this is consistent with the X-ray structure, in which the Met20 loop and nicotinamide ring are disordered (*8*). Favorable packing interactions between the nicotinamide and pterin rings increase the occupancy of the nicotinamide binding pocket and stabilize the closed conformation (*8*, *10*). Hence, the ternary complexes formed from folate and NADPH or $NADP^+$, or from DHF and $NADP^+$, in which both the pterin and nicotinamide rings are planar or nearly planar, adopt the closed conformation with both rings occupying the active site. By analogy, we also expect the E:DHF:NADPH Michaelis complex to

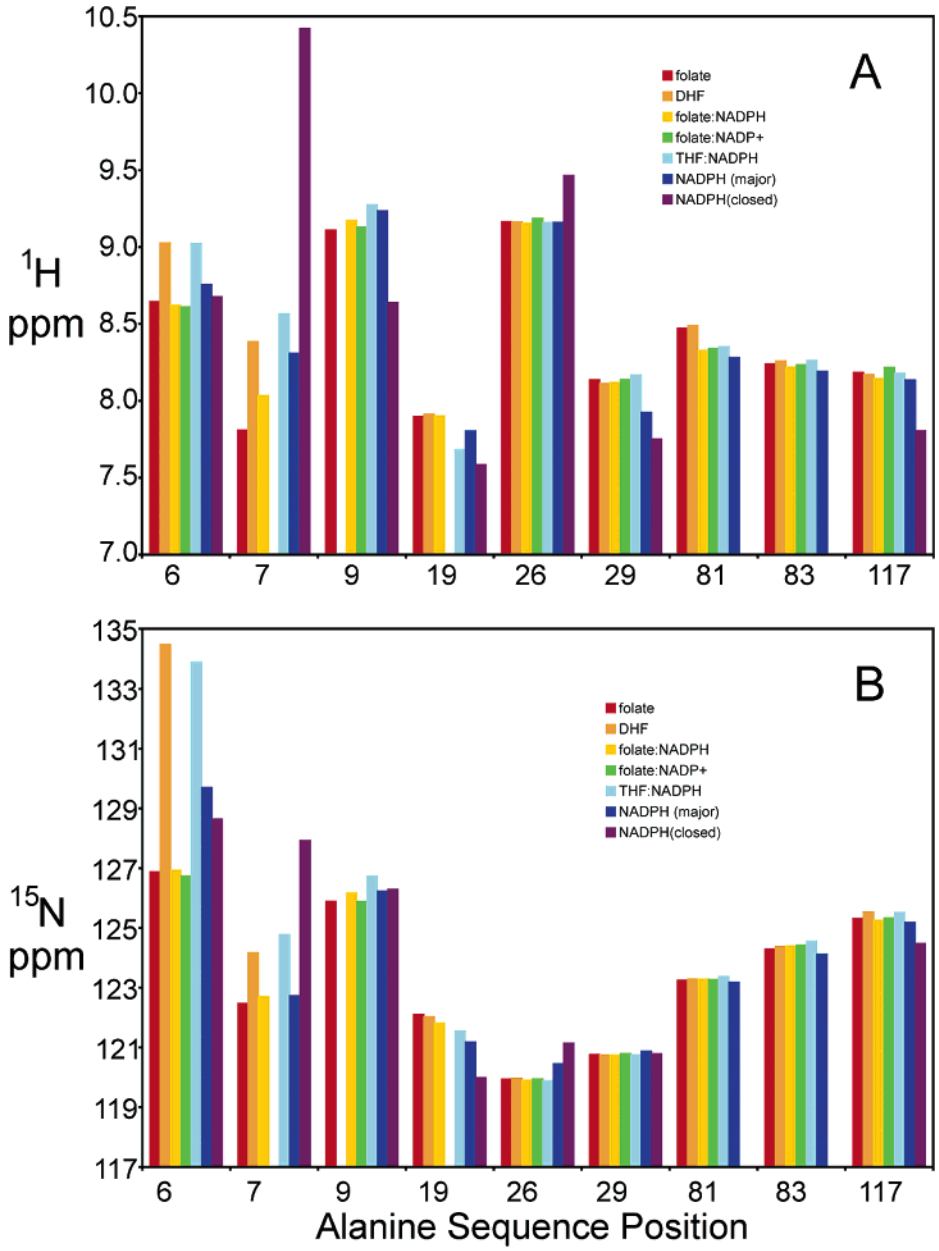

FIGURE 7: Histograms summarizing (A) ^{1}HN and (B) ^{15}N chemical shifts of alanine residues in G121V DHFR complexes. Complexes are represented by red, E:folate; orange, E:DHF; yellow, E:folate:NADPH; green, E:folate:NADP$^+$; light blue, E:THF:NADPH; dark blue, E:NADPH (major species, occluded); purple, E:NADPH (minor species, closed). All chemical shifts refer to spectra recorded at 282 K.

be closed. However, when either of the rings is strongly puckered, as in the ternary complexes containing DHNADPH or THF, the nicotinamide ring is excluded from the binding pocket and the active site loops adopt the occluded conformation. The driving force for this transition appears to be steric clash between the pterin and nicotinamide rings (*10*).

Loop Conformational Changes during the Catalytic Cycle. The NMR experiments reported here provide direct insights into the active site occupancy and loop conformations of all of the intermediates that participate in the catalytic cycle of *E. coli* DHFR. The results are summarized on the complete catalytic scheme in Figure 8 (*4*); the heavy arrows indicate the kinetic pathway (shown in Figure 1) for steady-state turnover under saturating substrate concentrations. The most notable feature is that the large amplitude conformational transitions between the closed and occluded conformations, with movements of backbone and side chain atoms by as much as 12 Å, are an integral part of the reaction cycle. While both the holoenzyme (E:NADPH) and the Michaelis complex (E:DHF:NADPH) adopt the closed conformation, all of the THF product complexes (E:THF:NADP$^+$, E:THF, and E:THF:NADPH) are occluded. Thus, the enzyme must cycle between the closed and the occluded states at two steps in the reaction cycle, immediately following hydride transfer and again after product release.

Loop Conformations in the G121V Mutant Enzyme. Substitution of Gly121 by valine and other bulky side chains has a dramatic effect on the kinetics of DHFR, decreasing the hydride transfer rate by up to 1000-fold and resulting in an additional kinetic step in the reaction mechanism (*23*). A recent molecular dynamics, CD, and fluorescence study of apoDHFR suggested that the G121V mutation may destabilize the contacts between the Met20 and FG loops and lead to some structural perturbation (*24*). To probe the effect of

Table 1: Conformational States of Wild-Type and G121V DHFR Complexes

complex[a]	wild-type DHFR	G121V DHFR
apoenzyme	disordered	disordered
E:folate	*occluded*	*occluded*
E:DHF	*occluded*	*occluded*
E:THF	*occluded*	nm[b]
E:NADPH	*closed*	*occluded (+closed)*[c]
E:NADP$^+$	*occluded*	nm
E:DHNADPH	disordered	nm
E:folate:NADP$^+$	disordered	*occluded*
E:folate:NADPH	*closed*	*occluded*
E:DHF:NADP$^+$	*closed*	nm
E:DHF:DHNADPH	*occluded*	nm
E:THF:NADP$^+$	*occluded*	*occluded*
E:THF:NADPH	*occluded*	*occluded*

[a] Intermediates in the steady-state cycle are in bold. Models for the Michaelis complex are in italic. [b] nm, not measured. [c] The predominant conformation for the E:NADPH complex of G121V is occluded, with a small population of the closed state present.

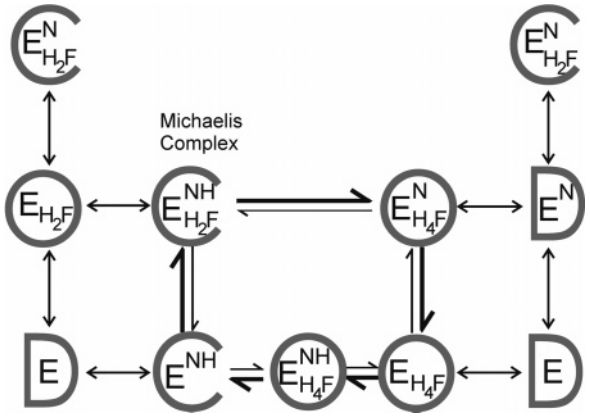

FIGURE 8: Complete kinetic scheme for DHFR (from ref *4*), showing active site loop conformations determined in the present NMR experiments. C, closed; O, occluded; D, disordered (multiple loop conformations).

the mutation on the conformation of DHFR in the various states formed during the reaction cycle, ^{1}H−^{15}N HSQC spectra of [^{15}N]alanine-labeled protein were recorded. With the sole exception of Ala9, which is close to the site of mutation, the ^{1}H−^{15}N HSQC spectrum (Figure 6A) of the folate complex of G121V DHFR is almost identical to that of the folate complex of the wild-type protein, allowing resonances to be assigned by inspection. [The assignments for this complex were confirmed through triple resonance experiments on the folate complex of uniformly ^{13}C,^{15}N-labeled DHFR G121V (B. Duggan and P. E. Wright, unpublished data).] The close similarity of the ^{1}HN and ^{15}N chemical shifts, in particular for the Ala117 marker resonances, confirms that the G121V DHFR complex with folate, like that of the wild-type enzyme, adopts the occluded conformation. Likewise, the spectra also indicate that the Met20 loop in the DHF binary complex and the THF:NADPH product release complex is in the occluded conformation in the mutant enzyme. However, a striking difference from wild-type behavior is observed for ternary complexes of G121V with folate and NADPH or NADP$^+$; in contrast to the closed E:folate:NADPH and E:folate:NADP$^+$ complexes of wild-type DHFR, the same complexes formed by the mutant enzyme (E:folate:NADP$^+$ shown in Figure 6B) are occluded. This is not due to inability to bind cofactor, since the marker resonances for binding of the adenosine moiety (Ala81 and Ala84) are at their characteristic positions for the cofactor-bound state.

The HSQC spectrum of the G121V DHFR holoenzyme, formed by addition of excess NADPH, reveals conformational heterogeneity (Figure 6C). Although the resonances of Ala81 and Ala84 confirm that the enzyme is fully bound by NADPH, the chemical shifts for the dominant conformer are similar to those for the folate complex and its conformation is clearly occluded. It is therefore likely that the nicotinamide ring is excluded from its binding pocket in this occluded conformer. Many of the weak secondary resonances have chemical shifts that correspond closely to those of the wild-type E:NADPH complex, confirming a minor population of a closed conformation formed by the G121V mutant. Direct evidence that the nicotinamide ring can access the binding pocket and hydrogen bond to Ala7 in the closed conformer comes from the large downfield shift observed for the Ala7 NH cross-peak, which occurs at a similar chemical shift to that of the wild-type E:NADPH complex. Finally, an additional very weak resonance can be observed for the well resolved signals from Ala6, Ala26, and Ala117, indicating formation of a very small population of a third conformational state that, based on its chemical shifts, appears to resemble the third conformer formed by wild-type DHFR bound to DHNADPH and the minor conformer present in the apoenzyme. A small population of this state is also present in the apo form of G121V DHFR.

The NMR spectra thus reveal a critical difference between G121V DHFR and the wild-type enzyme: the closed Met20 loop conformation is strongly destabilized in the mutant enzyme. In the wild-type enzyme, the E:folate:NADP$^+$ complex that mimics the Michaelis complex is fully closed, while the corresponding complex of the G121V mutant is occluded, with the population of the closed state being below the threshold for detection in ^{1}H−^{15}N HSQC experiments. Formation of the closed Michaelis complex is thus strongly disfavored in the mutant enzyme. Even in the NADPH binary complex of the G121V DHFR, in which the pterin binding pocket is empty, the dominant species in solution adopts the occluded Met20 loop conformation and only a small population of molecules form the closed conformer in which the nicotinamide-ribose moiety occupies its binding pocket in the active site. This destabilization of the closed form is attributed to steric effects of the substitution at Gly121. An examination of the X-ray structures of the closed folate:NADP$^+$ ternary complex (PDB 1rx2) and the occluded folate binary complex (PDB 1rx7) of wild-type DHFR shows that a bulky valine residue can be readily accommodated at this site when the enzyme is in the occluded conformation. However, because of steric clash with Val13, this bulky side chain at position 121 cannot be accommodated in the closed conformation of DHFR without some structural rearrangement.

The observed destabilization of the closed state of the G121V mutant provides a plausible explanation for the observed differences in kinetics relative to wild-type DHFR. Pre-steady-state kinetic analysis revealed a slow conformational change (at a rate of 3.5 s^{-1}) that precedes hydride transfer in the G121V mutant (*23*). On the basis of the present NMR experiments, it is expected that the initial complex formed between the holo E:NADPH form of G121V and

the DHF substrate would be in the occluded conformation, with the nicotinamide ring excluded from the active site. The slow conformational rearrangement observed in the kinetics probably reflects formation of an unstable "closed" state, in which the nicotinamide ring is inserted into its binding pocket adjacent to the pterin ring of the substrate. While our present experiments provide no direct insights into the origins of the substantial decrease in hydride transfer rate observed for the mutant protein (*23*), it is likely that the steric destabilization of the closed state might result in changes in active site geometry that would be manifest in the kinetics. Indeed, we note that recent quantum mechanical and molecular mechanical simulations suggest that the G121V mutation leads to an altered transition state structure, with a concomitant increase in the activation free energy barrier (*25*, *26*), and also perturbs the critical hydrogen-bonding interactions between the Met20 and FG loops (*27*).

ACKNOWLEDGMENT

We thank Drs. Jason Schnell and Jim Huntley for valuable discussions and Linda Tennant for technical assistance.

SUPPORTING INFORMATION AVAILABLE

^{1}H and ^{15}N chemical shifts for wild-type DHFR (Table S1) and G121V DHFR (Table S2). This material is available free of charge via the Internet at http://pubs.acs.org.

REFERENCES

1. Blakley, R. L. (1969) *The Biochemistry of Folic Acid and Related Pteridines*, Elsevier/North-Holland, Amsterdam.
2. Hitchings, G. H., Jr. (1989) Nobel lecture in physiology or medicine--1988. Selective inhibitors of dihydrofolate reductase, *In Vitro Cell Dev. Biol. 25*, 303−310.
3. Schnell, J. R., Dyson, H. J., and Wright, P. E. (2004) Structure, dynamics and catalytic function of dihydrofolate reductase, *Annu. Rev. Biophys. Biomol. Struct. 33*, 140.
4. Fierke, C. A., Johnson, K. A., and Benkovic, S. J. (1987) Construction and evaluation of the kinetic scheme associated with dihydrofolate reductase from *Escherichia coli*, *Biochemistry 26*, 4085−4092.
5. Andrews, J., Fierke, C. A., Birdsall, B., Ostler, G., Feeney, J., Roberts, G. C. K., and Benkovic, S. J. (1989) A kinetic study of wild-type and mutant dihydrofolate reductases from *Lactobacillus casei*, *Biochemistry 28*, 5743−5750.
6. Thillet, J., Adams, J. A., and Benkovic, S. J. (1990) The kinetic mechanism of wild-type and mutant mouse dihydrofolate reductases, *Biochemistry 29*, 5195−5202.
7. Matthews, D. A., Alden, R. A., Bolin, J. T., Freer, S. T., Hamlin, R., Xuong, N., Kraut, J., Poe, M., Williams, M., and Hoogsteen, K. (1977) Dihydrofolate reductase: X-ray structure of the binary complex with methotrexate, *Science 197*, 452−455.
8. Bystroff, C., Oatley, S. J., and Kraut, J. (1990) Crystal structures of *Escherichia coli* dihydrofolate reductase: The NADP+ holoenzyme and the folate. NADP+ ternary complex. Substrate binding and a model for the transition state, *Biochemistry 29*, 3263−3277.
9. Bystroff, C., and Kraut, J. (1991) Crystal structure of unliganded *Escherichia coli* dihydrofolate reductase. Ligand-induced conformational changes and cooperativity in binding, *Biochemistry 30*, 2227−2239.
10. Sawaya, M. R., and Kraut, J. (1997) Loop and subdomain movements in the mechanism of *Escherichia coli* dihydrofolate reductase: Crystallographic evidence, *Biochemistry 36*, 586−603.
11. Osborne, M. J., Schnell, J., Benkovic, S. J., Dyson, H. J., and Wright, P. E. (2001) Backbone dynamics in dihydrofolate reductase complexes: Role of loop flexibility in the catalytic mechanism, *Biochemistry 40*, 9846−9859.
12. Zaborowski, E., Chung, J., Kroon, G. J. A., Dyson, H. J., and Wright, P. E. (2000) Backbone H^N, N, C^α, C' and C^β assignments of the 19 kDa DHFR/NADPH complex at 9 °C and pH 7.6, *J. Biomol. NMR 16*, 349−350.
13. Osborne, M. J., Venkitakrishnan, R. P., Dyson, H. J., and Wright, P. E. (2003) Diagnostic chemical shift markers for loop conformation and cofactor binding in dihydrofolate reductase complexes, *Protein Sci. 12*, 2230−2238.
14. Miller, G. P., and Benkovic, S. J. (1998) Deletion of a highly motional residue affects formation of the Michaelis complex for *Escherichia coli* dihydrofolate reductase, *Biochemistry 37*, 6327−6335.
15. Osborne, M. J., and Wright, P. E. (2001) Anisotropic rotational diffusion in model-free analysis for a ternary-DHFR complex, *J. Biomol. NMR 19*, 209−230.
16. Delaglio, F., Grzesiek, S., Vuister, G. W., Guang, Z., Pfeifer, J., and Bax, A. (1995) NMRPipe: A multidimensional spectral processing system based on UNIX pipes, *J. Biomol. NMR 6*, 277−293.
17. Johnson, B. A., and Blevins, R. A. (1994) NMRView: A computer program for the visualization and analysis of NMR data, *J. Biomol. NMR 4*, 604−613.
18. Wishart, D. S., Bigam, C. G., Yao, J., Abildgaard, F., Dyson, H. J., Oldfield, E., Markley, J. L., and Sykes, B. D. (1995) ^{1}H, ^{13}C and ^{15}N chemical shift referencing in biomolecular NMR, *J. Biomol. NMR 6*, 135−140.
19. Muhandiram, D. R., and Kay, L. E. (1994) Gradient-enhanced triple-resonance three-dimensional NMR experiments with improved sensitivity, *J. Magn. Reson. Series B 103*, 203-216.
20. Falzone, C. J., Cavanagh, J., Cowart, M., Palmer, A. G., Matthews, C. R., Benkovic, S. J., and Wright, P. E. (1994) ^{1}H, ^{15}N and ^{13}C resonance assignments, secondary structure, and the conformation of substrate in the binary folate complex of *Escherichia coli* dihydrofolate reductase, *J. Biomol. NMR 4*, 349−366.
21. Li, L., Falzone, C. J., Wright, P. E., and Benkovic, S. J. (1992) Functional role of a mobile loop of *Escherichia coli* dihydrofolate reductase in transition-state stabilization, *Biochemistry 31*, 7826−7833.
22. Falzone, C. J., Wright, P. E., and Benkovic, S. J. (1994) Dynamics of a flexible loop in dihydrofolate reductase from *Escherichia coli* and its implication for catalysis, *Biochemistry 33*, 439−442.
23. Cameron, C. E., and Benkovic, S. J. (1997) Evidence for a functional role of the dynamics of glycine-121 of *Escherichia coli* dihydrofolate reductase obtained from kinetic analysis of a site-directed mutant, *Biochemistry 36*, 15792−15800.
24. Swanwick, R. S., Shrimpton, P. J., and Allemann, R. K. (2004) Pivotal Role of Gly 121 in Dihydrofolate Reductase from *Escherichia coli*: The Altered Structure of a Mutant Enzyme May Form the Basis of Its Diminished Catalytic Performance, *Biochemistry 43*, 4119−4127.
25. Watney, J. B., Agarwal, P. K., and Hammes-Schiffer, S. (2003) Effect of mutation on enzyme motion in dihydrofolate reductase, *J. Am. Chem. Soc. 125*, 3745−3750.
26. Thorpe, I. F., and Brooks, C. L., III (2003) Barriers to hydride transfer in wild type and mutant dihydrofolate reductase from E-coli, *J. Phys. Chem. B 107*, 14042−14051.
27. Rod, T. H., Radkiewicz, J. L., and Brooks, C. L., III (2003) Correlated motion and the effect of distal mutations in dihydrofolate reductase, *Proc. Natl. Acad. Sci. U.S.A. 100*, 6980−6985.

BI048119Y